MODE I DELAMINATION GROWTH IN ADHESIVELY BONDED JOINTS UNDER STATIC AND FATIGUE LOADS

by

Subodh C. Biswas

Shaik Jeelani

School of Engineering and Architecture

Tuskegee University

Tuskegee, AL 36088

Prepared for

NASA LANGLEY RESEARCH CENTER

GRANT NO. NAG-1-447

SEMI-ANNUAL REPORT

Abstract

The objective of this investigation was to characterize the pure mode I delamination growth in metal to metal adhesively bonded joints under static and fatigue loading conditions, using FM 73 adhesive.

Double cantilever beam specimens (DCB) were used for pure mode I tests. Aluminum 2024-T3 adherend were bonded with FM 73 adhesive. Delamination was introduced during fabrication by inserting a Teflon film between the two adherends.

The mode I strain energy release rate G_{I_c} was obtained directly from static DCB tests conducted in accordance with the ASTM designation D1876-12.

Constant amplitude fatigue tests on DCB specimens were conducted to determine the relationship between delamination growth rate da/dN and strain energy release rate G_{I_c}, for a pure mode I delamination growth.

It is found that the debond propagation rate in adhesive joints using FM 73 is more sensitive to errors in design load than is typical crack growth rate in metallic structures.

1. Introduction

The advantages of adhesively bonded joints over mechanically fastened joints has encouraged the aerospace industry to use the former in structural components and systems. Such joints produce lower stress concentration than the mechanically fastened joints and have high strength to weight ratio. Even with these potential advantages and encouraging experience with adhesive bonding, manufacturers still hesitate to use the technology in primary structural components. This is partly due to lack of understanding of failure mechanisms and durability. Several investigators (1-6) used the fracture mechanics concepts of strain energy release rate to model the failure of adhesively bonded joints. The total strain energy release rate, G_T, of an adhesive joint can be resolved into three components G_I, G_{II}, G_{III} associated with three debonding modes: I (opening), II (sliding), and III (tearing), respectively. However, in most practical applications, only G_I and G_{II}, due to peel and shear stresses, respectively, exist near the debond front. Everett (5) showed that the strain energy release rate associated with peel stresses had a significant effect on cyclic debonding.

The objective of this study was to characterize a pure mode I delamination growth in metal to metal adhesively bonded joints under static and fatigue loading conditions using FM 73 adhesive. The widely used double cantilever beam (DCB) specimens were used to characterize debond growth under opening mode I loading conditions. Aluminum 2024-T3 was used as adherend.

2. Fabrication of Test Specimens

The adherends were made from commercially available aluminum 2024-T3 sheets. Each adherend measured 1/8 inch x 1 inch in cross section and 8.5 inch in length. The adherends were bonded with FM 73 adhesive and BR 127 primer supplied by American Cyanamide. The surface preparation of the adherends and cure of the adhesive were performed as per the manufacturer's recommendations (7). A film of teflon was introduced to cause the desired initial delamination in the test specimens as shown in fig. 1. Hinges were attached at the end of the DCB specimens to make certain that there was no bending moment introduced in the adherend during loading.

3. Description of DCB Test

Static tests were conducted in a displacement-controlled mode. The test set up is shown in fig. 2. Stable delamination growth was achieved by controlling the tip of the displacement. Prior to mounting the specimen as shown in fig. 2, the side surface was coated with typewriter correction fluid so that visible marks could be made at the extent of delamination. Prior to recording the test data, the DCB specimens were loaded such that the length of the joint holding the teflon tape opened and introduced a sharply defined visible delamination. The initial delamination length was recorded with the help of a microscope held adjacent to the specimen.

Static tests were conducted according to the ASTM standard (8) at constant slow speeds to induce slow delamination growth. The load (P) corresponding to the applied displacement (δ) was also monitored. P increased linearly with δ when the delamination length (a) remained constant. This was continued until critical values (P_{cr}, δ_{cr}) were reached. When the tip displacement exceeded δ_{cr}, a delamination growth (Δa) was observed, accompanied by a reduction in the load from the P_{cr} value. The

applied displacement was then decreased until a zero load reading was observed. It may be noted that a zero load reading did not correspond to a zero displacement reading. The loading/unloading procedure was repeated for the growth of delamination. The slope of the load displacement plots indicated an increase in compliance with an increase in delamination size. The critical load and deflection values and the compliance measured corresponding to the delamination sizes were recorded during each static test. Plots of critical loads and compliance as a function of the delamination size were obtained and slopes of the curves were used to compute G_{I_c}, the mode I critical strain energy release rate. The computation procedure is explained in section 4.

Constant amplitude fatigue tests were conducted at a frequency of ω = 10 cycles and a stress ratio of R = 0.1. The maximum cyclic load was selected based on the static test data. Fatigue test specimens also had their side surface coated with typewriter correction fluid to aid the measurements. A microscope was used to monitor the delamination growth. The delamination size and the corresponding cycles were recorded at selected intervals. Delamination growth rate da/dN and its variation with delamination size (a) were obtained. Using available static test data these results were converted to da/dN versus G_{I_c} plots which are conventional delamination growth rate records.

4. Results and Discussion

Static double cantilever beam (DCB) tests were conducted to compute the strain energy release rate (G_I) for a pure mode I delamination growth. These displacement controlled tests produced load-displacement (P versus δ) curves similar to those shown in fig. 3. The compliances ($C = \delta/P$) of the DCB specimen were obtained from the slope of the curves in fig. 3.

Figure 4 shows the variation in the compliance with the delamination size. Figure 5 shows the variation in the critical load with delamination size. The slope of the fig. 4 (dc/da) was used to calculate the strain energy release rate for the DCB specimens. The strain energy release rate (G_I) for the pure mode I is calculated using the following equations.

$$G_{I_c} = \frac{P_{cr}^2}{2w} \frac{dc}{da}, \qquad \text{where } w = 1 \text{ inch} \qquad (1)$$

Table 1 shows the experimental data including the values of dc/da, G_{I_c}, and G_{I_c}/P.

Constant amplitude fatigue tests were conducted on DCB specimens at a stress ratio of 0.1 and a frequency of 10 HZ. The maximum load was selected based on the static test data. The delamination size and the corresponding number of cycles were monitored. The test data are shown in fig. 6. Delamination growth rate was calculated form the slope of this curve. Figure 7 shows dc/da versus a data obtained from the static tests on DCB specimens. Using fig. 7 dc/da and the strain energy release rate for pure mode I were calculated for the fatigue tests for the delamination size "a." Figure 8 shows the variation of delamination growth rate with the strain energy release rate for DCB specimens.

The straight line graph in fig. 8 may be represented by the following equation:

$$da/dN = K(G_I)^n \qquad (2)$$

where n is the slope of the line. The value of n is 4.4. This value is quite high when compared with typical values of n derived from applying equation 2 to fatigue crack growth in aluminum and steel alloys, where n

ranges from 1.5 to 3 (9). Steep slopes means that small changes in applied load causes a large change in debond growth rate. Thus the debond propagation rate in adhesive joints is more sensitive to design loads than is the case in metallic structures. The value of n found in this investigation compares well with that found in other investigations (1-6).

5. Conclusions

1. The value of n in adhesive joints is higher than the typical values found for aluminum and steel.
2. In adhesively bonded joints a small change in the design load causes a large change in debond growth rate.
3. The values of n found in this investigation compared with the results of previous investigations.

References

1. W. S. Johnson and S. Mall, "A fracture mechanics approach for designing adhesively bonded joints." NASA TM 85694, September 1983.
2. S. Mall, W. S. Johnson and R. A. Everett, "Cyclic debonding of adhesively bonded composites." NASA TM 84577, November 1982.
3. W. S. Johnson and P. D. Mangalgiri, "Investigation of fiber bridging in double cantilever beam specimens." NASA TM 87716, April 1086.
4. S. Mall and W. S. Johnson, "Characterization of mode I and mixed mode failure of adhesive bonds between composites adherends." Composites Materials Testing and Design, ASTM STP 893, J. M. Whitney edition, ASTM, PA, 1986, pp. 322-334.
5. R. A. Everett, Jr. "The role of peel stress in cyclic debonding." NASA TM 84504, June 1982.

6. R. L. Ramkumar, "Performance of a quantitative study of instability related delamination growth." NASA TM 166046.

7. Data product handbook, American Cyanamide Company, Polymer Division, Wayne, NJ 05470.

8. Standard test method for "Peel resistance of adhesives." ASTM designation D 1876-72.

9. D. Broek, "Elementary engineering fracture mechanics." 3rd edition, Martinus Nijhoff Publishers, Boston, 1982.

Table 1: Test Data

P	a	C	dc/da	G_{I_c}	G_{I_c}/P
65	1.623	0.00134	0.004	8.45	0.13
56	2.185	0.00334	0.005	7.84	0.14
50	2.674	0.00625	0.0065	8.125	0.1625
46	2.95	0.00875	0.0083	8.78	0.19
45	3.216	0.0132	0.01	10.125	0.225
42	3.55	0.0156	0.011	9.702	0.231
38	3.872	0.0208	0.0135	9.747	0.2565
37	4.133	0.025	0.016	10.952	0.296
36	4.317	0.0291	0.018	11.664	0.324
33	4.574	0.0219	0.0225	12.25	0.371
33	4.844	0.0396	0.027	14.7015	0.4455
32	5.042	0.047	0.041	20.992	0.656
32	5.184	0.052	0.052	25.6	0.7875

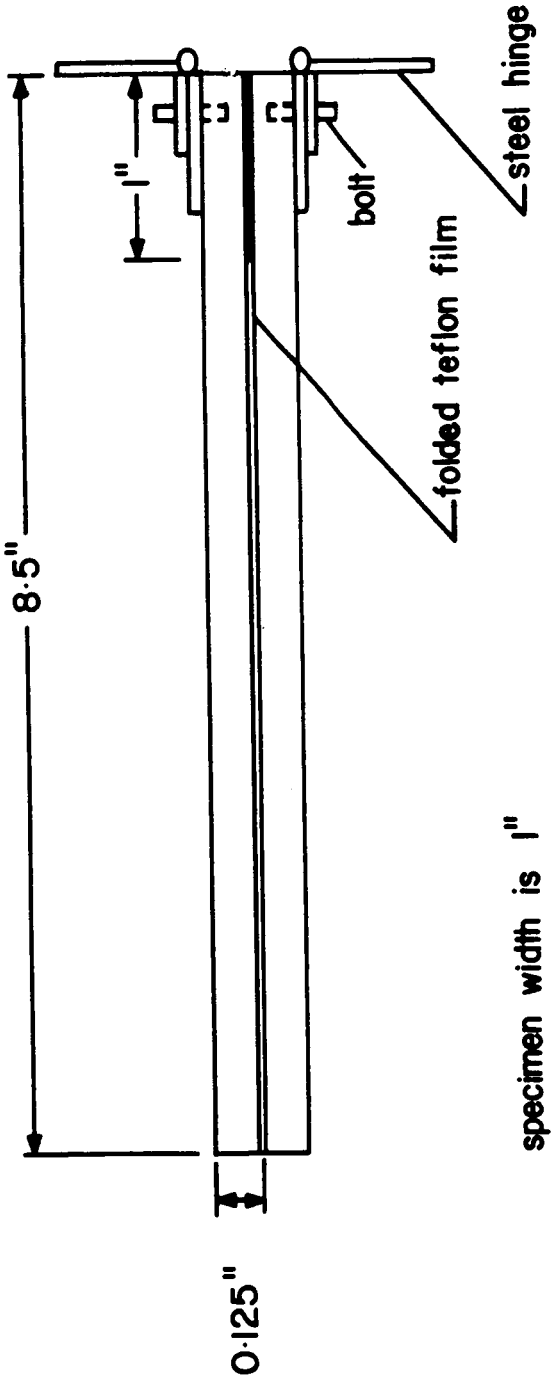

Fig. 1: Double Cantilever Beam (DCB) test Speciemens.

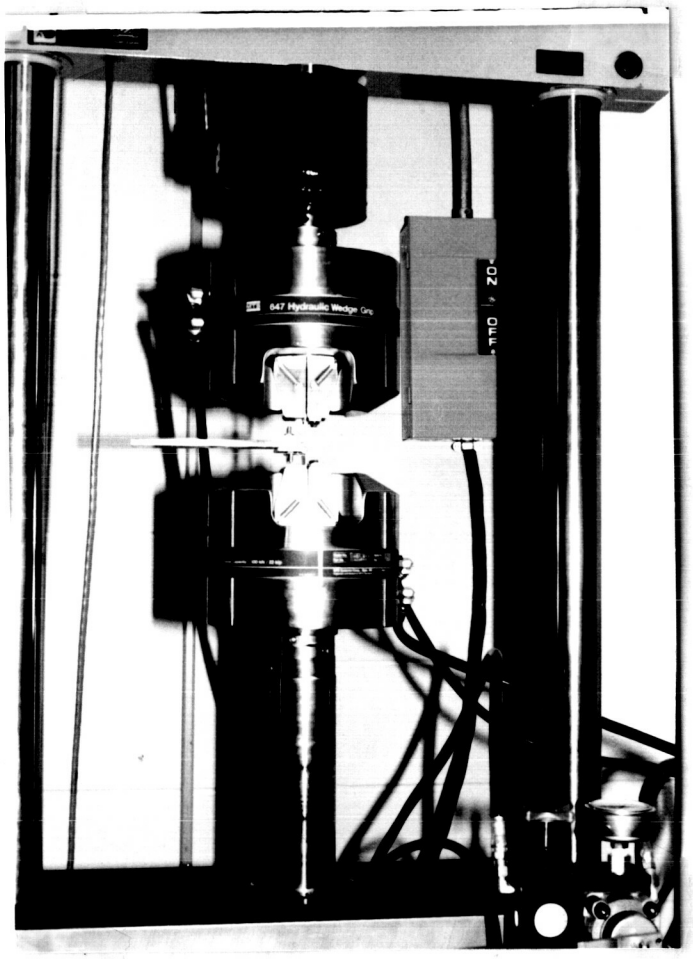

Fig. 2: Test Set-up

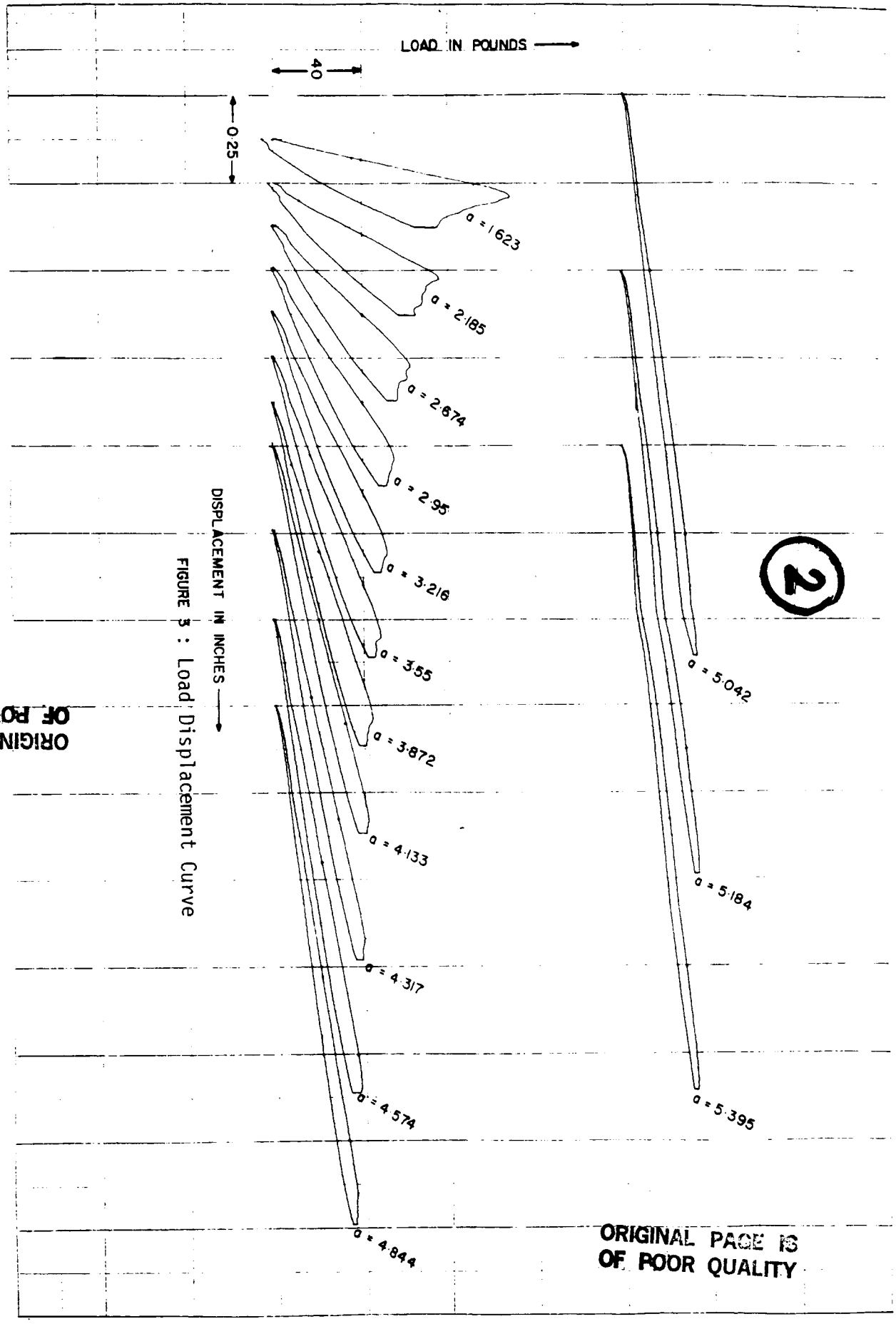

FIGURE 3 : Load Displacement Curve

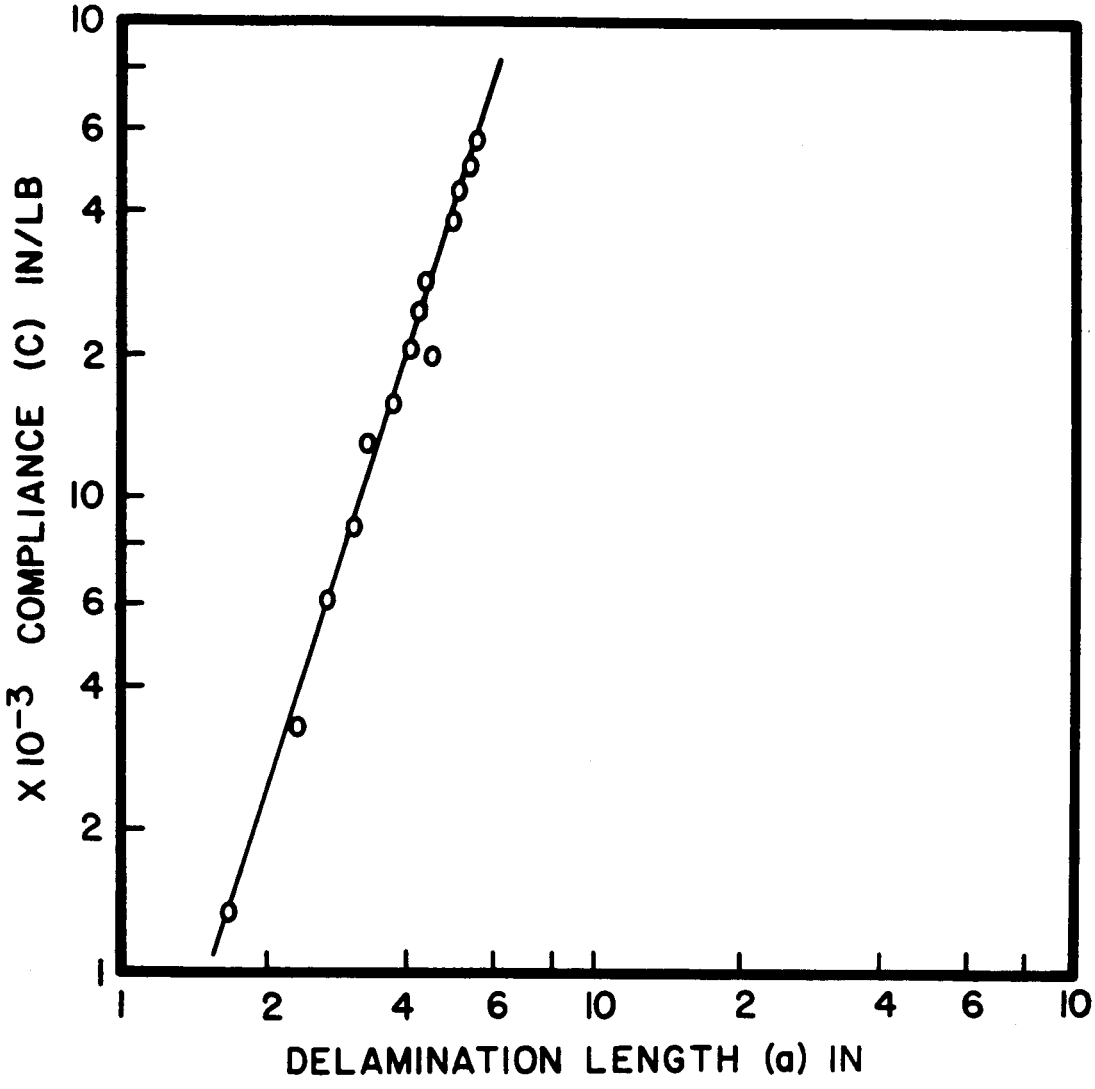

Fig. 4: Variation of Compliance with Delamination length.

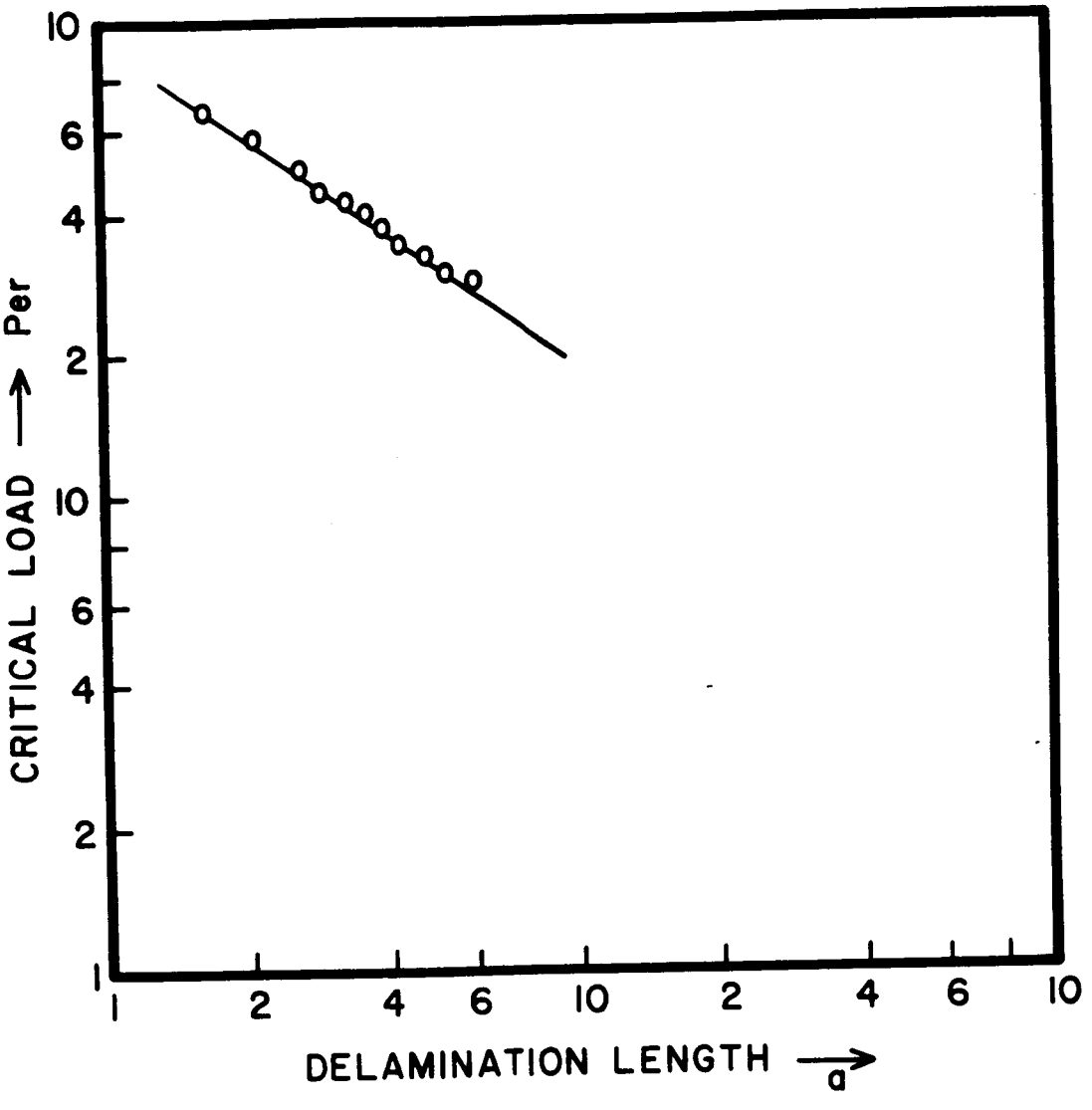

Fig 5: Variation of Critical load with Delamination length.

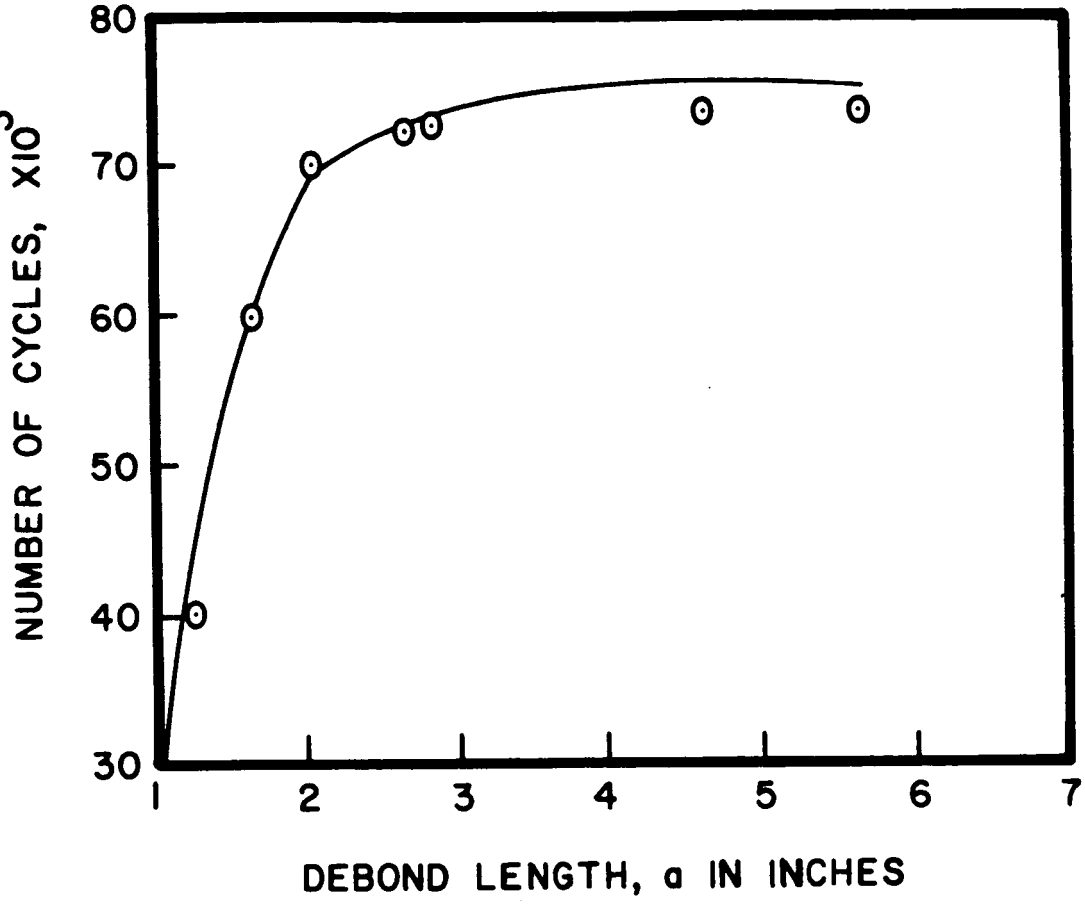

Fig. 6: Variation of Debond length "a" with Number of Cycles.

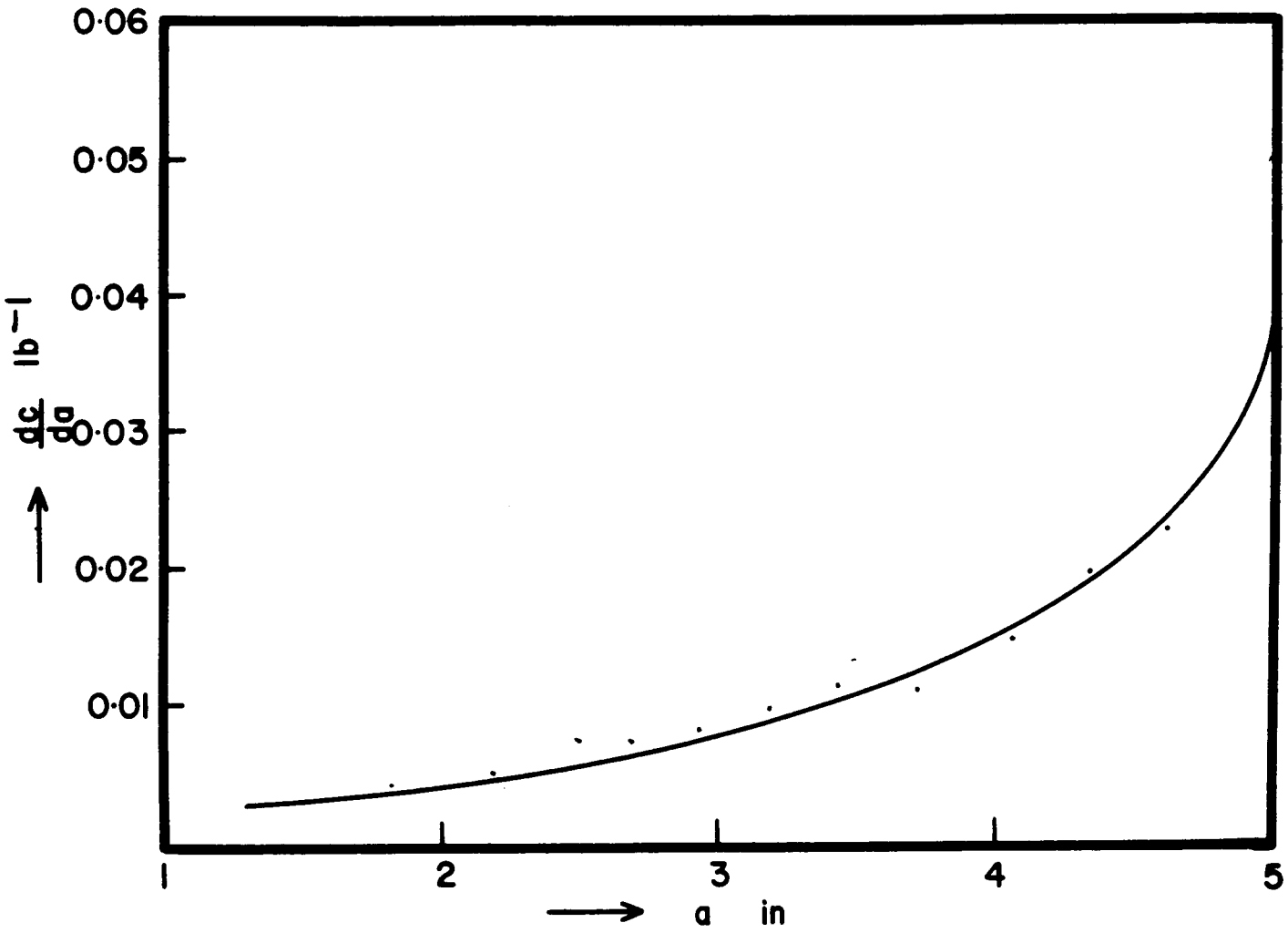

Fig. 7: Variation of Delamination length "a" with dc/da.

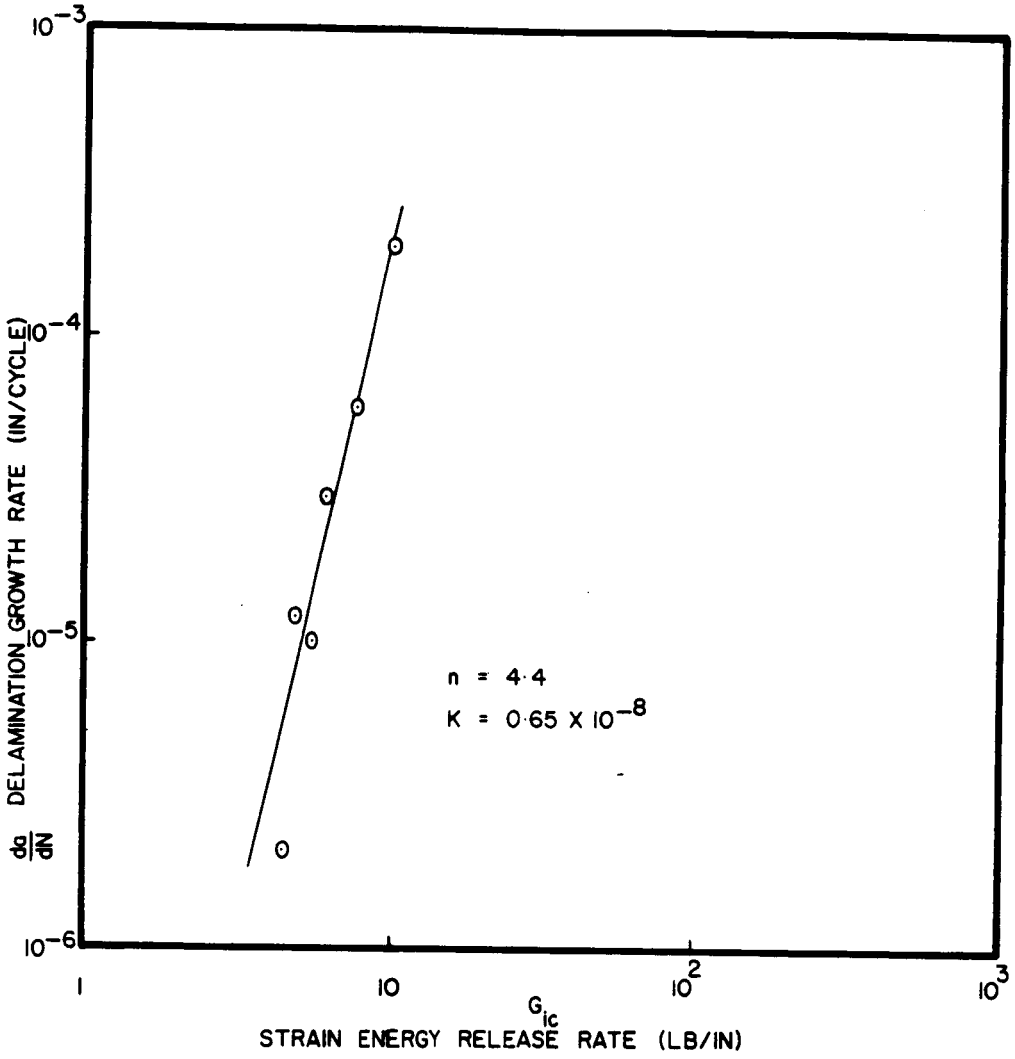

Fig. 8: Variation of Strain energy release rate with Delamination growth rate.